

## Fabrication of polysulfone/carbon nanospheres ultrafiltration membranes for removing some dyes from aqueous solutions

Hany Mohamed Abbas<sup>a</sup>, Rasha M. Kamel<sup>b</sup>, Mohamed E.A. Ali<sup>c\*</sup>, Aly H. Atta<sup>b</sup>, Hassan M.A. Hassan<sup>b,d</sup>, Ahmed Shahat<sup>b</sup>

<sup>a</sup>General Management of Chemical and Research Laboratories, Suez Oil Processing Company, Suez, Egypt

<sup>b</sup>Department of Chemistry, Faculty of Science, Suez University, Suez, Egypt

<sup>c</sup>Egyptian Desalination Research Center of Excellence (EDRC) & Hydrogeochemistry Department, Desert Research Center, Cairo, 11753, Egypt, Tel. +(02)01144098296; email: mohamedea@edrc.gov.eg (M.E.A. Ali)

<sup>d</sup>Chemistry Department, College of Science, Jouf University, P.O. Box: 2014, Sakaka, Saudi Arabia

Received 1 March 2020; Accepted 6 April 2020

### ABSTRACT

Carbon nanosphere particles (CNs) were prepared from glucose using a controlled hydrothermal and then used as fillers for polysulfone (PS) ultrafiltration (UF) membrane matrix. The prepared CNs, PS, and polysulfone/carbon nanosphere (PS/CNs) composite UF membranes were characterized by scanning electron microscope, X-ray diffraction, and water contact angle. Methyl blue and Rhodamine B dyes were used as feed solutions to elucidate the performance efficiency of the membranes. The adsorption properties of CNs, oxygen functional groups, and high surface area showed a significant improvement in the performance of the membranes against dyes removal. Because of CNs act as fillers, the membrane permeability decrease from 42.2 to 10.9 L/m<sup>2</sup> h bar for PS/CNs (7%). By addition the CNs, dye rejection increased from 51.4% to 93.6%, and from 39.3% to 81.5%, for Methyl blue and Rhodamine B dyes, respectively. While, the water flux decreased from 216.3 to 168.9 L/m<sup>2</sup>h 629 and from 409.6 L/m<sup>2</sup>h for the neat PS and PS/CNs (5%), respectively. The high rejection of Methyl blue than that of Rhodamine B was due to the difference in the molecular weight of the two dyes and the charged groups for dyes.

*Keywords:* Carbon nanospheres; Nanocomposite; Ultrafiltration membrane; Dye removal

### 1. Introduction

Enormous amounts of wastewater that contains harmful natural buildups are produced from color assembling forms, paper, food, material manufacture, and makeup as a colorant, annually approximately about 700,000 metric tons of dyes are produced via industries worldwide [1,2]. A large portion of the colors are poisonous and cancer-causing and are resistant to degradation by ordinary treatment steps because of their complex fragrant ring structure [3]. There are many purification techniques available like biological

treatment, physical and chemical methods for the evacuation of dyes, all of them have features and drawbacks [4]. Filtration has been considered as a promising sanitization innovation because of its simple technique, low energy consumption, environmentally safe and good efficiency, manufactured membranes are partitioned under organic (polymeric), inorganic, and hybrids of these two [5–9]. The membrane is a barrier layer between two phases, in which the particles greater than the pores are rejected and the littler ones penetrated. In the membrane separation method, the vast majority of the polymeric layers have been

\* Corresponding author.

Presented at the 4th International Water Desalination Conference: Future of Water Desalination in Egypt and the Middle East, 24–27 February 2020, Cairo, Egypt

1944-3994/1944-3986 © 2020 Desalination Publications. All rights reserved.

set up by the phase inversion process. A homogeneous polymer arrangement is given a role as a thin film mixed with nanomaterial and submerged into a coagulation bath [10]. Between casting solution and non-solvent, the diffusional exchange of solvent and non-solvent can make the casting solution phase-separate to form a membrane [11]. Over the last three decades nanoparticles have received an increasing amount of research interest. This is due to the unique size-dependent properties of nanoparticles, which are often thought of as a separate and intermediate state of the matter lying between individual atoms and bulk material. Recently, polymer nanocomposites emerged as one of the most promising developments in the area of membrane fabrication. The Polymer/nano-inorganic particles composite membranes present an interesting approach for improving the physical and chemical, as well as separation properties of polymer membranes because they possess characteristics of both organic and inorganic membranes such as good permeability, selectivity, mechanical strength, thermal stability and so on. CNs prepared by different carbon sources like glucose, xylose, sucrose, and derived saccharides at low temperatures [12]. The number and size of pores in membrane and properties of nano-particle which fill these pores play an important role in separation methods [13–17].

In this work, CNs were prepared from glucose using a hydrothermal synthesis method (green-chemistry), low temperatures in the HTC method obtain nano-sized carbon sphere have a good dispersion in membrane pores. PSf/PVP/CNs membrane was prepared by simple dispersing of CNs into polysulfone casting solution, the prepared membrane for dye removal by filtration system using the stirred cell to research the effect of concentration of CNs on permeate fluxes, morphology structures, and dyes rejection of the neat polysulfone membranes.

## 2. Experimental

### 2.1. Materials

Analytical grade glucose (Sigma-Aldrich, USA, MW = 180.16), ethanol (analytical grade, VWR, France), deionized (DI) water produced by the LaboStar PRO TWF ultra-pure water systems, 0.055  $\mu\text{S}/\text{cm}$  conductivity (18.2 M $\Omega\text{cm}$  resistivity) at 25°C, polysulfone beds (Udel P 3500 LCD MP7, MW = 77000, Mn = 22000), polyvinylpyrrolidone (PVP), N, N-dimethylformamide (DMF), Methyl blue and Rhodamine B were purchased from Sigma-Aldrich.

### 2.2. Synthesis of carbon nanosphere (CNs)

Carbone nanospheres were synthesized, in term of a green-chemistry method, by low heat treatment of glucose according to hydrothermal processes [18–22]. In brief, 4 g of glucose was being dissolved in 60 ml of DI water and then kept in a 100 ml Teflon lined autoclave and heated at 180°C for 6 h. Then, the autoclave was cooled and the product was rinsed in ethanol and dried at 60°C for 5 h.

### 2.3. Preparation of PS and PS/CNs ultrafiltration membranes

The neat PS and PS/CNs composite membranes were prepared by using the phase inversion technique [23,24].

In brief, PS casting solution was prepared by dissolving 15 wt.% of PS and 4 wt.% of PVP (as pore former) in DMF at 80°C–90°C with continuous stirring for 6 h. Then, the solution was left at room temperature for 24 h to be degassed, before the casting the mixture was gently re-mixed to assure the homogeneity of the mixture. The resultant solution was then cast on a cleaned surface of a glass plate using a doctor blade knife to achieve a membrane thickness of  $\sim 200 \mu\text{m}$ , and then coagulated in a DI water bath. After about 10 min of gelation, the resulting PS membrane was removed from the gelation bath and washed with DI water to remove the residual DMF and pore formation. The same previous method was used for the preparation of PS/CNs membrane, where different amounts of CNs nanoparticles (0–1 wt.%) were firstly dispersed in DMF, the mixture was undergone to ultrasonic for about 30 min with an operating frequency of 30 kHz to ensure a high degree of CNs dispersion, after that PVP and PS were added to the mixture and then cast as illustrated before. The membranes were coded as M0 to M7 depending on the content of CNs, Table 1. All of the prepared membranes were kept in DI water for 24 h before use.

### 2.4. Characterization

The morphological structure of the membranes and CNs were observed using a scanning electron microscope (FESEM, ZEISS SEM ultra 60,5KV). The composite membrane samples were coated with gold before the section images of the membranes. The microstructure of the membranes and CNs were studied by X-ray diffraction (XRD) Siemens D5000 powder diffractometer Cu  $K_{\alpha}$  radiation (wavelength  $\lambda = 0.15406 \text{ nm}$ ) with a nickel filter at 40 kV and 30 mA. The contact angle of the membranes was calculated by using contact angle analyzer, high-pressure chamber by Biolin Scientific.

### 2.5. Membranes performance evaluation

The performance of the membranes against dye rejection was carried out using a stirred cell filtration system connected to a nitrogen gas cylinder (stirred cell, HP4750, cell diameter of 5.1  $\text{cm}^2$ , and processing volume of 300 ml, the effective filtration membrane area was 14.6  $\text{cm}^2$ ), Fig. 1. The pure water permeability of the membranes was tested

Table 1  
Composition of the different casting solutions

Membrane	PSf (g)	CNs Mass (g)	PVP (g)	DMF (g)
M0	15	0	4	81
M0.5	15	0.075	4	80.925
M1	15	0.15	4	80.85
M2	15	0.3	4	80.7
M3	15	0.45	4	80.55
M4	15	0.6	4	80.4
M5	15	0.75	4	80.25
M6	15	0.9	4	80.1
M7	15	1.05	4	79.95

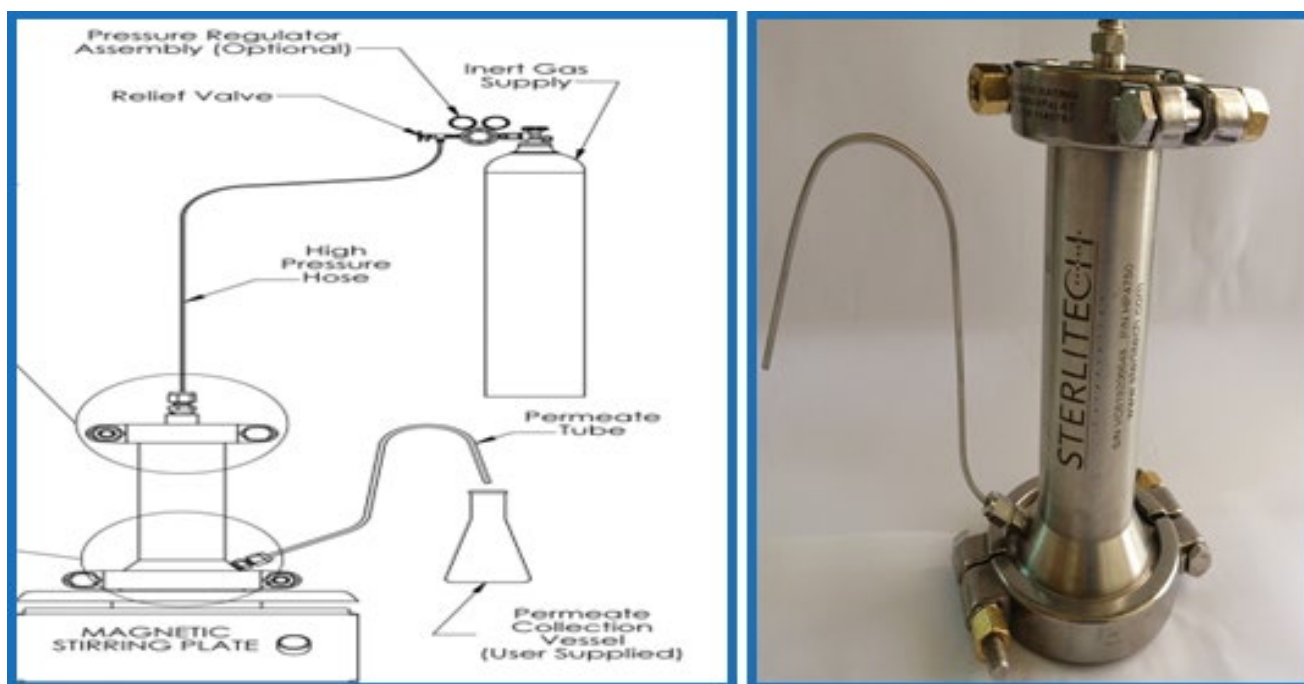


Fig. 1. Schematic diagram of the filtration system and Stirred cell HP4750.

at different applied pressures ranged from 1 to 5 bar. The volume flux was calculated as follow:

$$J_v = \frac{V}{At}$$

where  $J_v$  permeate flux ( $L/m^2h$ ),  $V$  is the volume of permeate solution collected (L),  $A$  is the effective membrane area ( $m^2$ ) and  $t$  is time (h) [25]. Permeation flux test of dyes was carried out using 10 ppm Methyl blue and 10 ppm Rhodamine b, their chemical structure are shown in Fig. 2. The experiments were carried out by running filtration cycles and collecting 50 mL aliquots of each dye solution for each, after that the concentrations were monitored using an Acculab UVS-90. UV-vis spectrophotometer at wavelengths of 594 and 554 nm, respectively, the rejection was calculated as follows;

$$R = \left( 1 - \frac{C_p}{C_f} \right) \times 100\%$$

where  $R$  is the rejection (%),  $C_p$  and  $C_f$  are the concentrations of the permeate and feed solutions, respectively.

### 3. Results and discussions

#### 3.1. Characterization

It was found that CNs were successfully prepared by using a hydrothermal reaction of glucose at a low temperature of  $190^\circ C$ . The microstructure and morphology of the samples were observed at different two magnifications using SEM, Figs. 3a and b. Carbon nano-spheres were

prepared by hydrothermal carbonization (HTC) glucose, in the range of 50–400 nm. Based on many experiments, not shown here, the heat treatment of hydrothermally synthesized CNs by using glucose gave the good properties, surface morphology yield and reduce the particle size, which made it disperse very well in the polysulfone casting solution. Glucose arrangement was kept in a 100 mL Teflon lined autoclave and warmed for 6 h at  $190^\circ C$ . It was, firstly, broken down into hydroxymethyl-furfural, and afterward continuous polymerization–polycondensation with the development of little cores has been carried out. These cores developed as indicated by the Lamer model until every one of the “monomers” has been expended and the last molecule size was achieved. The temperature plays a significant role in determining the quantity of surface oxygen groups, the number of oxygen groups decreased as the temperature increased, an examination of oxygen substance and O/C proportions showed further carbonization, and was directly related to temperature, so by expanding hydrothermal procedures time or temperature (over  $190^\circ C$ ) prompts an expansion in breadth of CNs since more atoms can arrive at the focal center lead to an increase in diameter of carbon and extra-enormous size over 500 nm in distance across which is not of our interest at this time, so CNs are mass materials without significant porosity [26–28].

Fig. 3 displays SEM micrographs of PS, PS/PVP, and PS/CNs nanocomposite membranes with different contents of CNs. The polysulfone membrane was found to be somewhat porous (Fig. 3c), but as PVP was applied, a highly porous membrane with clear pores was created (Fig. 3d). It is recognized that the addition of PVP improves the formation of a pore in polymer membranes and enhances their permeation properties; it is a strong pore-forming agent and anti-biofouling agent by giving enough time to

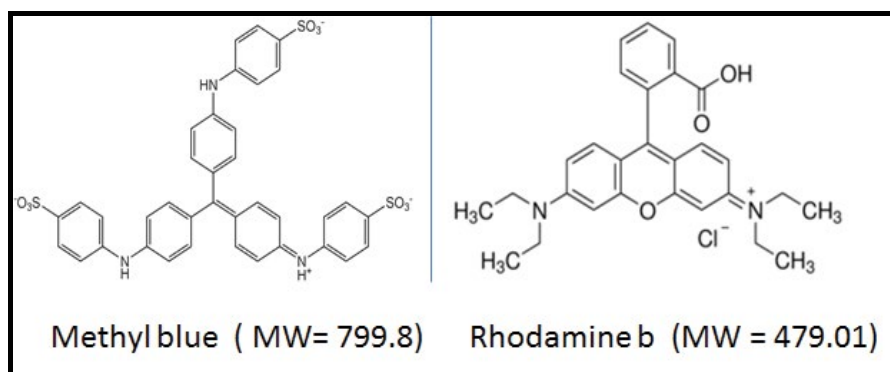


Fig. 2. Chemical structure of the organic dyes.

accumulate and shape a dense layer of polysulfone molecules. The number of pores and the porosity of the prepared membrane are therefore found to be increased [29–31]. The changes in membrane morphology as a result of adding CNs are shown dramatically as it fills the membrane pores (Figs. 3e–h). As the CNs in the polymer casting solution increased from 0.5% to 7%, the surface structure of PS appears to have changed significantly. As a consequence, the CNs penetrated the surface of the membrane and accumulated in the pores, the diffusion through the surface pores occurs because the particles are small enough (50–400 nm) to escape the size exclusion, through the nanoparticles to try to fill all the pores to provide high density. The inclusion of CNs would improve the properties of electrical, thermal, and surface adsorption [32–34]. In order to be well mixed and evenly distributed throughout the polymer matrix even at the highest concentration, the rejection of dyes by surface adsorption properties has increased [35].

XRD analysis was studied to obtain further information about the effect of CNs on the physicochemical properties of PS membranes, Fig. 4. The X-ray diffraction patterns of CNs exhibited a shoulder band at  $2\theta = 16.5^\circ$  and a main broad one at  $2\theta = 21^\circ$ , which indicates a significant level of topological disorder in the sample during the preparation process. The presence of no other detected peaks supports the amorphous nature of the CNs sample and the random organization with no specific geometry of the nanoparticles [36,37]. The X-ray diffraction of PS/CNs blended membrane shows the same broadband with a little shift, which confirm the existence of CNs in the polymeric network of the membrane and small peak sharper in presence PVP act as pore former [21].

The measurement results of the water contact angle of PS and its composites with CNs membranes are shown in Fig. 5. It is clear that, contact angle values showed a gradual decrease from  $83.3^\circ$  of PS membrane to  $61.2^\circ$ . This gradual decrease indicates an increase in hydrophilicity of the membranes due to the surface oxygen groups (–OH and –C=O) that produce low temperature (HTC) processes in the CNs [36,37].

### 3.2. Membranes performance

The membrane permeability of the PS ultrafiltration membranes was gradually decreased as CNs concentration

increases in the casting solution from 0.5 to 7 wt.%, Fig. 6. This was clearly seen since the permeability decrease from  $42.2 \text{ L/m}^2 \text{ h bar}$  for PS membrane to  $10.9 \text{ L/m}^2 \text{ h bar}$  for PS/CNs 7%. This is because pure polysulfone casting solution produced a thinner and more porous membrane, consequently provided a higher hydraulic permeability, as CNs were added it affects the pore structure of the membranes either by deposition in therein or increasing the membrane thickness. As the thickness of membrane support increased, the membrane becomes denser and the presence of sponge-like structure has reduced the rate of water permeability through the membranes.

Fig. 7 shows the effect of CNs onto the water flux and rejection of organic dyes. It can be seen that while the rejection of the two dyes was gradually increased with increasing CNs content, the water flux was shown to be decreased. From the figure there is a difference in the performance of the membranes against the two dyes. For Methyl blue dye, the rejection increased from 51.4% to 93.6% with a gradual decrease of water flux from  $216.3$  to  $168.9 \text{ L/m}^2 \text{ h}$  for the neat PS and PS/CNs (5%), respectively. On the other hand, in the case of Rhodamine B, the rejection increased from 39.3% to 81.5%, while the flux decreased from 629 to  $409.6 \text{ L/m}^2 \text{ h}$ . The high rejection of Methyl blue than that of Rhodamine B is due to the difference in the molecular weight of the two dyes and the charged groups for dyes [35,38,39]. In other words, Donnan exclusion and sieve mechanism depended on the pore size and solute diameter played an important role in the membranes performance. CNs size and shape affected the rate of dye rejection and permeation flux, as it prepared with small size consequently had a high surface area, adsorption of dyes was significant.

## 4. Conclusions

Carbon nanospheres were successfully synthesized using a green-chemistry method by the hydrothermal decomposition of glucose in the water at low heat treatment ( $190^\circ\text{C}$ ). It was used at different concentrations (0.5%–7%) as fillers for polysulfone (PS) ultrafiltration membrane, which prepared by phase inversion technique. The adsorption properties of CNs, oxygen functional groups, and high surface area, showed a significant improvement in the performance of the membranes against dyes removal. Methyl blue and Rhodamine B dyes were used as feed solutions to elucidate

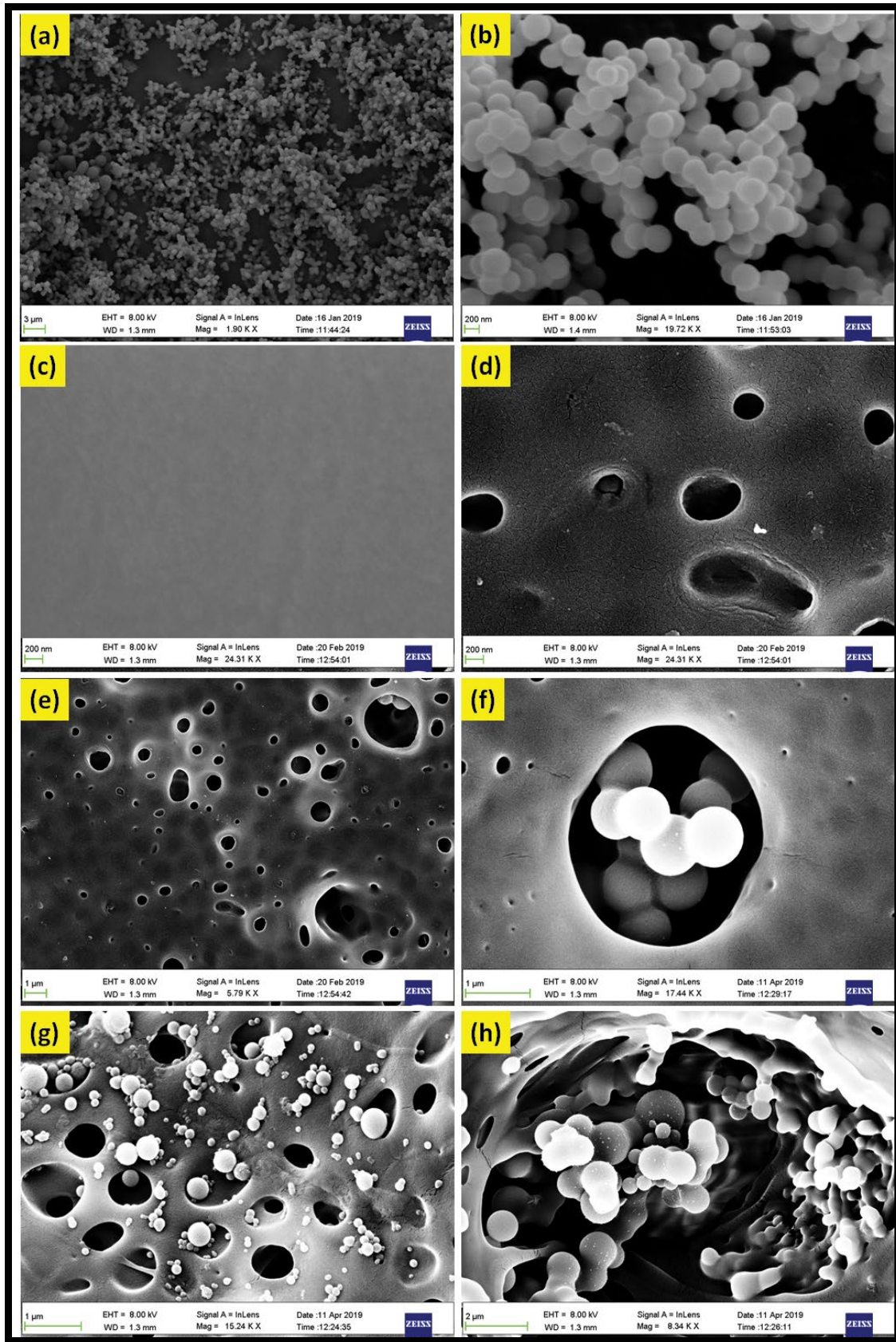


Fig. 3. SEM surface images of (a and b) CNs, (c) PS, (d) PS/PVP, (e) PS/CNs<sub>0.5r</sub>, (f) PS/CNs<sub>5r</sub>, (g) PS/CNs<sub>6r</sub>, and (h) PS/CNs<sub>7r</sub>.

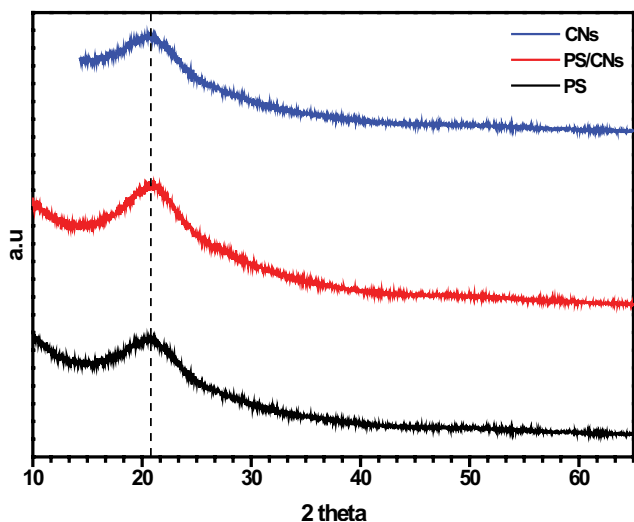


Fig. 4. XRD patterns of PS/PVP, CNs, and PS/CNs membranes.

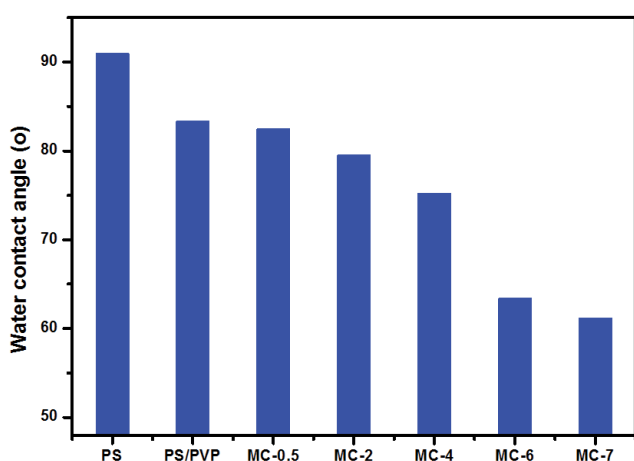


Fig. 5. Effect of CNs concentration on the contact angle of the membranes.

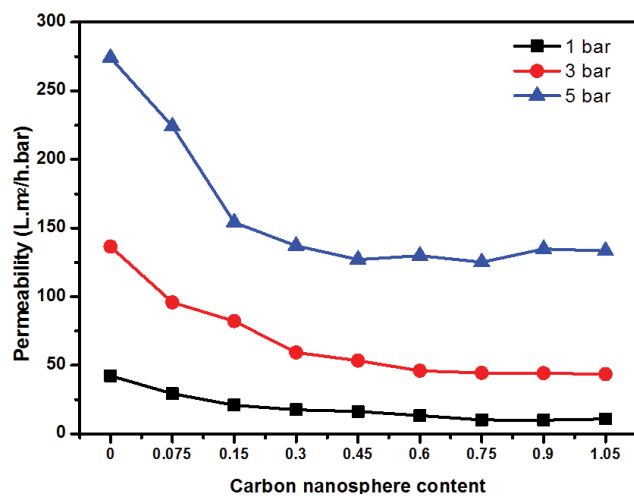


Fig. 6. Membranes permeability at different pressures as a function of CNs content.

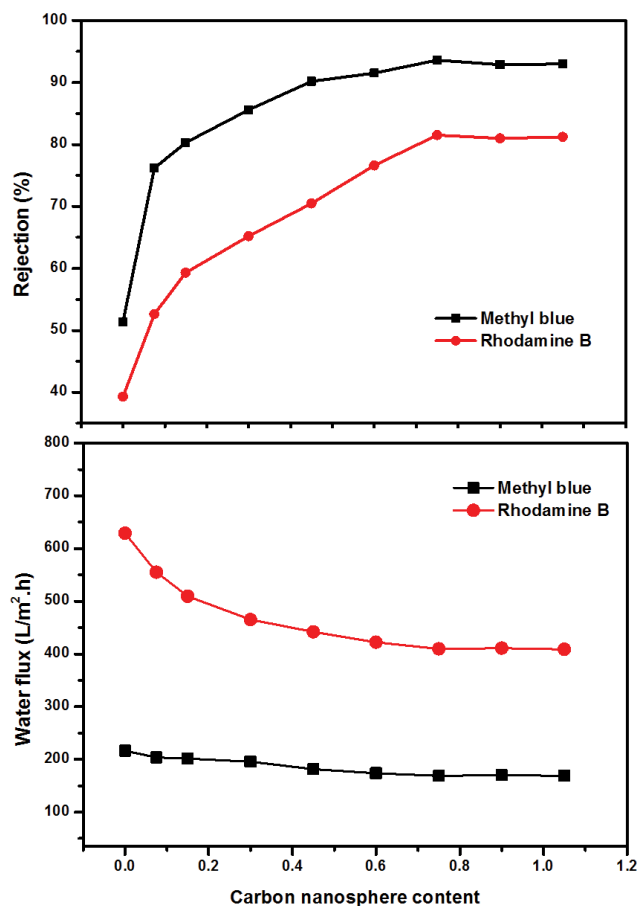


Fig. 7. Water flux and rejection of Methyl blue and Rhodamine B dyes.

the performance efficiency of the membranes. Because of CNs act as fillers, the membrane permeability decreases from 42.2 L/m<sup>2</sup> h bar for PS membrane to 10.9 L/m<sup>2</sup> h bar for PS/CNs (7%). The results revealed that for Methyl blue dye, the rejection increased from 51.4% to 93.6% with a gradual decrease of water flux from 216.3 to 168.9 L/m<sup>2</sup> h for the neat PS and PS/CNs (5%), respectively. On the other hand, in the case of Rhodamine B, the rejection increased from 39.3% to 81.5%, while the flux decreased from 629 to 409.6 L/m<sup>2</sup> h. The high rejection of Methyl blue than that of Rhodamine B was due to the difference of the molecular weight of the two dyes and the charged groups for dyes.

## References

- [1] M. Santhi, P. Kumar, B. Muralidharan, Removal of Malachite green dyes by adsorption onto activated carbon-MnO<sub>2</sub>-nanocomposite-kinetic study and equilibrium isotherm analysis, *IOSR J. Appl. Chem.*, 8 (2015) 33-41.
- [2] V. Garg, R. Kumar, R. Gupta, Removal of Malachite green dye from aqueous solution by adsorption using agro-industry waste: a case study of *Prosopis cineraria*, *Dyes Pigm.*, 62 (2004) 1-10.
- [3] D. Shen, J. Fan, W. Zhou, B. Gao, Q. Yue, Q. Kang, Adsorption kinetics and isotherm of anionic dyes onto organo-bentonite from single and multisolute systems, *J. Hazard. Mater.*, 172 (2009) 99-107.

- [4] E. Daneshvar, M. Kousha, M. Jokar, N. Koutahzadeh, E. Guibal, Acidic dye biosorption onto marine brown macroalgae: isotherms, kinetic and thermodynamic studies, *Chem. Eng. J.*, 204 (2012) 225–234.
- [5] J. Cadotte, R. Forester, M. Kim, R. Petersen, T. Stocker, Nanofiltration membranes broaden the use of membrane separation technology, *Desalination*, 70 (1988) 77–88.
- [6] H. Te Hennepe, D. Bargeman, M. Mulder, C. Smolders, Zeolite-filled silicone rubber membranes: part 1: membrane preparation and pervaporation results, *J. Membr. Sci.*, 35 (1987) 39–55.
- [7] H.-T. Yeo, S.-T. Lee, M.-J. Han, Role of a polymer additive in casting solution in preparation of phase inversion polysulfone membranes, *J. Chem. Eng. Jpn.*, 33 (2000) 180–184.
- [8] R. Boom, I. Wienk, T. Van den Boomgaard, C. Smolders, Microstructures in phase inversion membranes, part 2: the role of a polymeric additive, *J. Membr. Sci.*, 73 (1992) 277–292.
- [9] M.R. Esfahani, S.A. Aktij, Z. Dabaghian, M.D. Firouzjaei, A. Rahimpour, J. Eke, I.C. Escobar, M. Abolhassani, L.F. Greenlee, A.R. Esfahani, Nanocomposite membranes for water separation and purification: fabrication, modification, and applications, *Sep. Purif. Technol.*, 213 (2018) 465–499.
- [10] J. Aburabie, L.F. Villalobos, K.V. Peinemann, Composite membrane formation by combination of reaction-induced and nonsolvent-induced phase separation, *Macromol. Mater. Eng.*, 302 (2017) 1700131.
- [11] M. Di Luccio, R. Nobrega, C. Borges, Microporous anisotropic phase inversion membranes from bisphenol-a polycarbonate: study of a ternary system, *Polymer*, 41 (2000) 4309–4315.
- [12] P. Karna, M. Ghimire, S. Mishra, S. Karna, Synthesis and characterization of carbon nanospheres, *Open Access Lib. J.*, 4 (2017) 1–7.
- [13] B.S. Lalia, V. Kochkodan, R. Hashaikheh, N. Hilal, A review on membrane fabrication: structure, properties and performance relationship, *Desalination*, 326 (2013) 77–95.
- [14] J.T. Jung, J.F. Kim, H.H. Wang, E. Di Nicolo, E. Drioli, Y.M. Lee, Understanding the non-solvent induced phase separation (NIPS) effect during the fabrication of microporous PVDF membranes via thermally induced phase separation (TIPS), *J. Membr. Sci.*, 514 (2016) 250–263.
- [15] M. Rezakazemi, M. Sadrzadeh, T. Mohammadi, T. Matsuura, Methods for the Preparation of Organic-Inorganic Nanocomposite Polymer Electrolyte Membranes for Fuel Cells, D. Inamuddin, A. Mohammad, A. Asiri Eds., *Organic-Inorganic Composite Polymer Electrolyte Membranes*, Springer, Cham, 2017, pp. 311–325.
- [16] M. Rezakazemi, M. Sadrzadeh, T. Matsuura, Thermally stable polymers for advanced high-performance gas separation membranes, *Prog. Energy Combust. Sci.*, 66 (2018) 1–41.
- [17] F. Liu, N.A. Hashim, Y. Liu, M.M. Abed, K. Li, Progress in the production and modification of PVDF membranes, *J. Membr. Sci.*, 375 (2011) 1–27.
- [18] K. Pan, H. Ming, Y. Liu, Z. Kang, Large scale synthesis of carbon nanospheres and their application as electrode materials for heavy metal ions detection, *New J. Chem.*, 36 (2012) 113–118.
- [19] X. Sun, Y. Li, Colloidal carbon spheres and their core/shell structures with noble-metal nanoparticles, *Angew. Chem. Int. Ed.*, 43 (2004) 597–601.
- [20] A. Raza, J. Wang, S. Yang, Y. Si, B. Ding, Hierarchical porous carbon nanofibers via electrospinning, *Carbon Lett.*, 15 (2014) 1–14.
- [21] P. Zhang, Z.-A. Qiao, S. Dai, Recent advances in carbon nanospheres: synthetic routes and applications, *Chem. Commun.*, 51 (2015) 9246–9256.
- [22] M. Li, Q. Wu, M. Wen, J. Shi, A novel route for preparation of hollow carbon nanospheres without introducing template, *Nanoscale Res. Lett.*, 4 (2009) 1365.
- [23] R.J. Gohari, W. Lau, T. Matsuura, E. Halakoo, A. Ismail, Adsorptive removal of Pb(II) from aqueous solution by novel PES/HMO ultrafiltration mixed matrix membrane, *Sep. Purif. Technol.*, 120 (2013) 59–68.
- [24] A.R. Hassan, S. Rozali, N.H.M. Safari, B.H. Besar, A.R. Hassan, S. Rozali, N.H.M. Safari, B.H. Besar, The roles of polyethersulfone and polyethylene glycol additive on nanofiltration of dyes and membrane morphologies, *Environ. Eng. Res.*, 23 (2018) 316–322.
- [25] H. Matsuyama, T. Maki, M. Teramoto, K. Kobayashi, Effect of PVP additive on porous polysulfone membrane formation by immersion precipitation method, *Sep. Sci. Technol.*, 38 (2003) 3449–3458.
- [26] X. Wang, C. Hu, Y. Xiong, C. Zhang, Synthesis of functional carbon nanospheres by a composite-molten-salt method and amperometric sensing of hydrogen peroxide, *J. Nanosci. Nanotechnol.*, 13 (2013) 933–936.
- [27] L.-H. Zhang, Q. Sun, C. Yang, A.-H. Lu, Synthesis of magnetic hollow carbon nanospheres with superior microporosity for efficient adsorption of hexavalent chromium ions, *Sci. China Mater.*, 58 (2015) 611–620.
- [28] K. Hemmati Kahradeh, E. Saievar-Iranizad, A. Bayat, Investigation of hydrothermal process time on the size of carbon micro- and nano-spheres, *J. Optoelectron. Nanostruct.*, 2 (2017) 51–60.
- [29] A.M. Telford, M. James, L. Meagher, C. Neto, Thermally cross-linked PNPV films as antifouling coatings for biomedical applications, *ACS Appl. Mater. Interfaces*, 2 (2010) 2399–2408.
- [30] Q. Qin, Z. Hou, X. Lu, X. Bian, L. Chen, L. Shen, S. Wang, Microfiltration membranes prepared from poly (N-vinyl-2-pyrrolidone) grafted poly (vinylidene fluoride) synthesized by simultaneous irradiation, *J. Membr. Sci.*, 427 (2013) 303–310.
- [31] B. Chakrabarty, A. Ghoshal, M. Purkait, Preparation, characterization and performance studies of polysulfone membranes using PVP as an additive, *J. Membr. Sci.*, 315 (2008) 36–47.
- [32] J. Zhang, Z. Xu, W. Mai, C. Min, B. Zhou, M. Shan, Y. Li, C. Yang, Z. Wang, X. Qian, Improved hydrophilicity, permeability, antifouling and mechanical performance of PVDF composite ultrafiltration membranes tailored by oxidized low-dimensional carbon nanomaterials, *J. Mater. Chem. A*, 1 (2013) 3101–3111.
- [33] Q. Li, S. Pan, X. Li, C. Liu, J. Li, X. Sun, J. Shen, W. Han, L. Wang, Hollow mesoporous silica spheres/polyethersulfone composite ultrafiltration membrane with enhanced antifouling property, *Colloids Surf., A*, 487 (2015) 180–189.
- [34] M.F. De Volder, S.H. Tawfik, R.H. Baughman, A.J. Hart, Carbon nanotubes: present and future commercial applications, *Science*, 339 (2013) 535–539.
- [35] K. Rambabu, S. Velu, Modified cellulose acetate ultrafiltration composite membranes for enhanced dye removal, *Int. J. Chem. Sci.*, 14 (2016) 195–205.
- [36] M. Li, W. Li, S. Liu, Control of the morphology and chemical properties of carbon spheres prepared from glucose by a hydrothermal method, *J. Mater. Res.*, 27 (2012) 1117–1123.
- [37] N. Zhang, X.Y. Cui, X.J. Zhao, Y.H. Zhou, H.M. Kan, Preparation of Nanometer Carbon Spheres by Hydrothermal Synthesis Method, in: *Key Engineering Materials*, Publisher in Material Science & Engineering, Trans Tech Publications Ltd., 2012, pp. 257–260.
- [38] S. Allen, B. Koumanova, Decolorization of water/wastewater using adsorption, *J. Univ. Chem. Technol. Metall.*, 40 (2005) 175–192.
- [39] D.D. Salman, W.S. Ulaiwi, N. Tariq, Determination the optimal conditions of Methylene blue adsorption by the chicken egg shell membrane, *Int. J. Poult. Sci.*, 11 (2012) 391–396.